

STM Study on Two-Dimensional Electronic System Localized on Surfaces*

Yukio Hasegawa

Institute for Materials Research (IMR), Tohoku University and Precursory Research for Embryonic Science and Technology (PRESTO), Japan Science and Technology Corporation (JST), 2-1-1 Katahira, Aoba-ku, Sendai, 980-77 JAPAN

In-Whan Lyo[†] and Phaedon Avouris

IBM T.J. Watson Research Center, Yorktown Heights, NY USA

(Received January 21, 1997)

There are some surface electronic states which can be regarded as two dimensional electronic system. Their properties have been studied using novel techniques of scanning tunneling microscopy (STM). Two examples of such surfaces; Si(111)7x7 structure and Au(111), are presented. It was found that behavior of electrons in such states are strongly affected by chemical (adsorbates) and morphological (steps or islands) properties of the surfaces.

KEYWORDS: surface states, two dimensional electron system, scanning tunneling microscopy, point contact, scanning tunneling spectroscopy

1. Introduction

For more than 30 years, surface science has revealed that surfaces of single crystals have different properties from those of bulk.¹⁾ For instance, in order to reduce the number of dangling bonds and surface energy, atomic arrangement on surfaces is reconstructed, exhibiting a superstructure. Electronic structure of surfaces is also modified accordingly because the periodicity of atomic arrangement in bulk is terminated at surfaces. As a result of those structural and electronic modifications, some surfaces possess electronic states which are localized on the surface and form a two dimensional electronic system, showing unique properties. A typical example of such surfaces is the Si(111)7x7 surface. Being a semiconductor, silicon has a band gap around the Fermi level. But, on this surface, because of its unique structure of dimer-adatom-stacking fault (DAS) model,²⁾ surface electronic states are formed within the band gap. It has been well-known that the states originating from the adatoms on the surface is so-called "metallic",³⁾ its energy level is located just on the Fermi level of the surface and the states are partially filled with electrons. Since the adatoms are located on the surfaces and their energy level is isolated from those of the bulk, the adatom states can be regarded as two dimensional (2D) electronic states localized on the surface.

In principle, this two dimension electron system localized on surfaces is different from the conventional system formed by space charge layer at semiconductor hetero interfaces like that of AlGaAs and GaAs.⁴⁾ The surface 2D system is intrinsic to the surface properties. No dopant is required and, thus, scattering by dopants, which is one of the factors limiting mean free path of the conventional 2D electronic system, does not have to be considered. Since it is confined within one or a few topmost layers of surfaces, it is ultimate and ideal in terms of its dimensionality. Because of this strong localization on the surface, its behavior can be modified and controlled

on a nanometer scale by arranging the steps and/or adsorbates on the surface, as was beautifully demonstrated by Crommie et al.⁵⁾ Its electron density is in an order of atomic density; $\sim 10^{14}/\text{cm}^2$, higher than that of conventional ones. Because of these differences, the surface 2D system may overcome the limitation of the conventional one and provide us new scheme of devices in the near future.

In this paper, two examples of the surface 2D electronic system are presented. One is for semiconductor surface, the Si(111)7x7 surface, as is already mentioned above, and the other is for metal; Au(111) and Cu(111) surfaces. Both surfaces have been studied by novel techniques using scanning tunneling microscopy (STM) operated under ultra-high vacuum (UHV) conditions.

2. Surface state conductivity of the Si(111)7x7 surface

The Si(111)7x7 surface is one of the most studied surfaces and its structural and electronic properties have been revealed using various techniques. The DAS model proposed by Takayanagi et al.²⁾ is a widely accepted structural model and there are 12 adatoms in a unit cell of the 7x7 structure. As for electronic properties, the surface is known to be "metallic" based on spectroscopic studies,³⁾ which means that there are surface states at the Fermi level. Since the Fermi level is positioned within the band gap of the bulk and they are attributed to the dangling bonds of the adatoms, the states are localized on surface. The problem is, however, that the adatoms are separated each other by 7Å and that no dispersion in the adatom electronic states has been observed using angle-resolved photoemission spectroscopy (ARPES). But, a quasi-elastic peak is observed in electron energy loss spectra (EELS),⁶⁾ which indicates that electrical conductivity exists in the surface states in a high frequency mode⁷⁾. Thus, there are some kinds of electrical connection among the adatoms on the

*IMR report No. 2082

surface, but so far electrical conductivity of the surface states has not been measured or detected in a direct way. In fact, so far electrical conductivity via surface states has never been measured on any surfaces⁸⁾ except the present study⁹⁾ and a recent study of electrical conductivity on Si(111)- $\sqrt{21}\times\sqrt{21}$ Ag by Hasegawa et al..¹⁰⁾

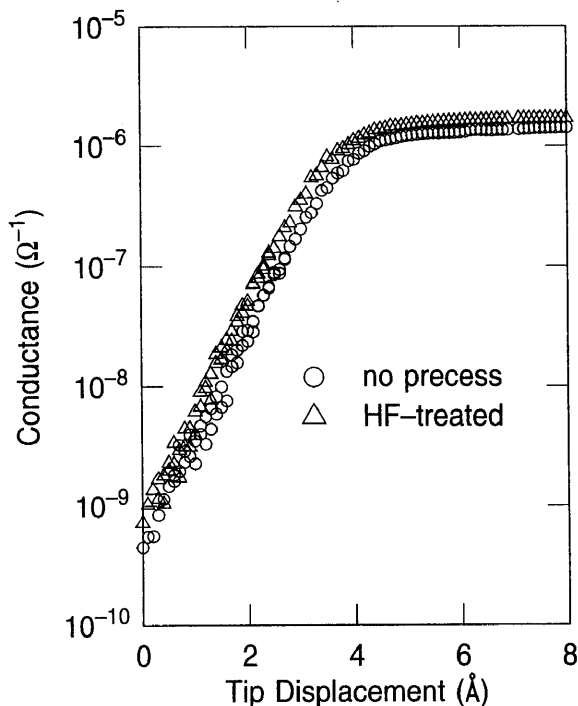


Fig. 1: Electrical conductance at $V=0$ between the tip and sample from the tunneling regime to contact. Starting from a position of normal STM condition, the tip was moved toward the sample, and conductance measured during the movement was plotted as a function of the tip displacement. At the beginning conductance increases exponentially with a decrease of the gap distance, and then it is saturated after contact formation.

In this chapter, we will present our effort trying to measure the surface state conductivity using STM. In our study, we use the tip of STM as a probe of electrical conduction of the sample. Taking an advantage of a high controllability of the gap distance between the tip and sample surface, we made a point contact of the tip on the surface with a nanometer-size contact area. An estimated diameter of contact area is less than 100\AA . Because of the small contact area and Schottky barrier formed at the metal (tip) - semiconductor (silicon) interface, electrical conduction through the contact area into the bulk is limited (less than $10^{-12}\Omega^{-1}$) and smaller than a leakage current which goes through the edge of the contact area. Based on the following experimental evidences, we conclude that a conductance through surface states is a dominant component in the leakage current at the point contact, and that it can be studied by a measurement of electrical conductance at a point contact. Actually, a component of electrical conduction through the interface also appears in the I-V spectra measured at contact. At contact, the spectra show strong rectification whose forward direction depends on a type of the dopant of the semiconductor samples. It can be explained by the Schottky barrier formation. However, the conductance of this component around $V=0$ is quite small

(less than $10^{-12}\Omega^{-1}$), negligible compared with the leakage component or the surface state component.

First of all, we measured the conductance on clean Si(111)7x7 surface. By applying a proper voltage on a piezo actuator which controls the tip position perpendicular with respect to the surface, we advanced the tip toward the silicon surface and made a point contact on it. From a start of the tip advancing to the contact formation, electrical conductance and I-V spectrum was measured.¹¹⁾ On the Si(111)7x7 surface, measured conductance (at $V=0$) at contact is found to be about $10^{-6}\Omega^{-1}$. An important thing to note here is that the conductance does not depend on the contact area as far as it is in nano-meter range. The measured conductance is, thus, quite reproducible. Typical examples of the conductance measurement is shown in Fig. 1. In this figure, conductance at $V=0$ is plotted as a function of tip displacement from a normal STM gap distance. In the tunneling regime, where the tip displacement is small and thus it is still separated with the surface, the conductance increases exponentially with the decrease of the gap distance (see logarithmic scale of the vertical axis), but around a contact, the conductance starts to be saturated and stays constant about $10^{-6}\Omega^{-1}$. Although this plot is cut at 8\AA of the tip displacement in Fig. 1, it was found that the saturation is kept at a displacement as much as 20\AA . The conductance at contact does not depend on a type of dopant of the samples. Both n-type and p-type doped silicon samples showed similar contact conductance as far as the 7x7 structure is formed on surface although their I-V spectra show opposite rectification. This indicates that the conductance is not a bulk component like the one due to space charge layer formation. The conductance does not depend on the tip material, either. We used tungsten and aluminum tips for this experiments and found no difference in terms of electrical conductance. These observations are all consistent with the model that the contact conductance is surface sensitive and probably due to surface state conductivity.

In order to check whether the conductance is due to the surface state conductivity, we investigated the effect of oxygen adsorption on the contact conductance. Oxygen atoms adsorb on the surface and make a bond with an adatom, reducing the density of the adatom states. If the measured conductance is due to the surface state conductivity, it should be reduced with oxygen adsorption. Our experimental results agree with this prediction as is shown in Fig. 2. Figure 2(top) is an STM image of oxygen adsorbed Si(111)7x7 structure. The amount of oxygen exposure is about 0.5L. Bright and dark dots are observed in this image which correspond to two kinds of adsorbates of oxygen on the surface.¹²⁾ We made a point contact on this kind of oxygen adsorbed Si(111)7x7 surfaces and measured the conductance. Figure 2(bottom) is a plot of the contact conductance during an oxygen exposure. It decreases exponentially with the amount of oxygen exposure down to $10^{-9}\Omega^{-1}$. Our experimental results show that the conductance drops as much as 3 orders of magnitude by less than 1ML of oxygen adsorption. This extreme sensitivity of the oxygen adsorption to the contact conductance indicates that the conductance is related with the topmost surface layer and probably surface state conductivity. We studied the effect of oxygen using Si samples with both types of dopant and did not find any dependence, which also rejects the possibility that it is due to bulk conductivity.

on a island increases again and finally reaches to that measured on flat area. This presumably indicates that by the further pushing the contact area becomes larger and the tip starts to make contact with terrace surrounding the island.

We have shown, in this chapter, that on the Si(111)7x7 surface there exists electrical conduction through the adatom states, that it is measurable by a point contact method using STM, and that it is modified by chemical and morphological properties around the contact area.

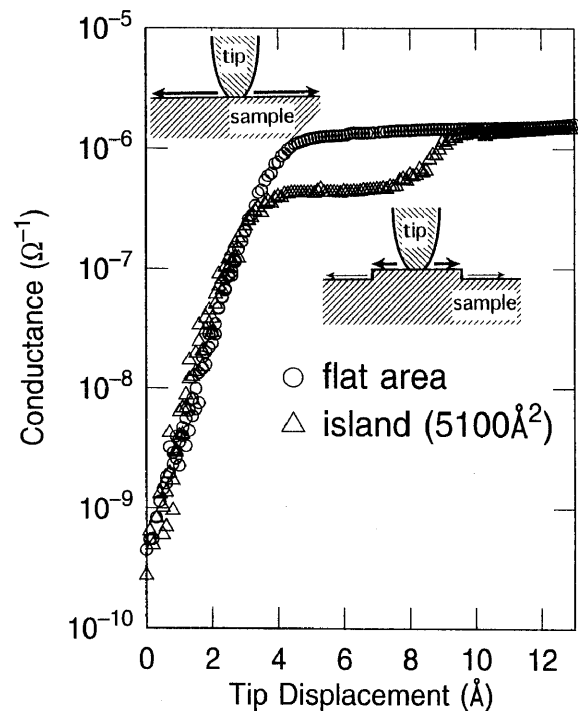
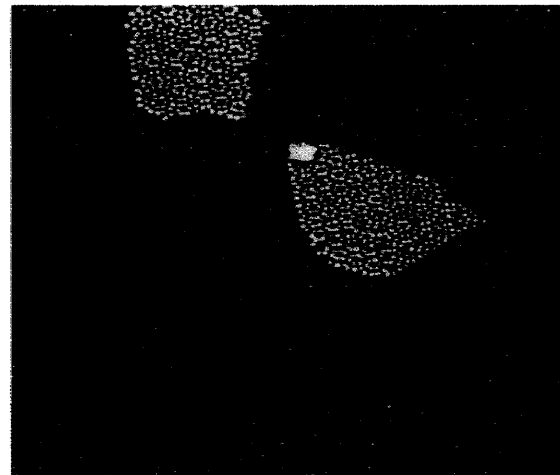


Fig. 3: (top) STM image of the Si(111)7x7 surface with Si islands. The size of observed area is about $600 \text{\AA} \times 600 \text{\AA}$. (bottom) A plot of conductance as a function of tip displacement from a normal tunneling position. Two curves measured on island and on terrace are compared.

3. Electron scattering on Au(111) and Cu(111) surfaces

In the previous chapter, we showed that steps on the surface have a significant effect on the electronic conduction via surface states. Here in this chapter, we

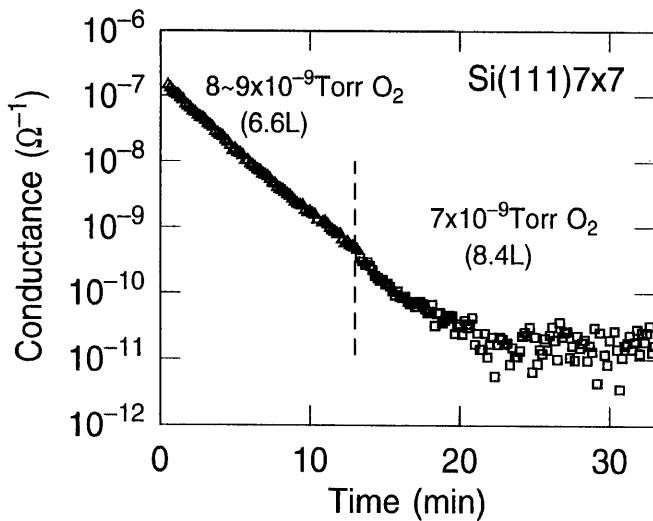
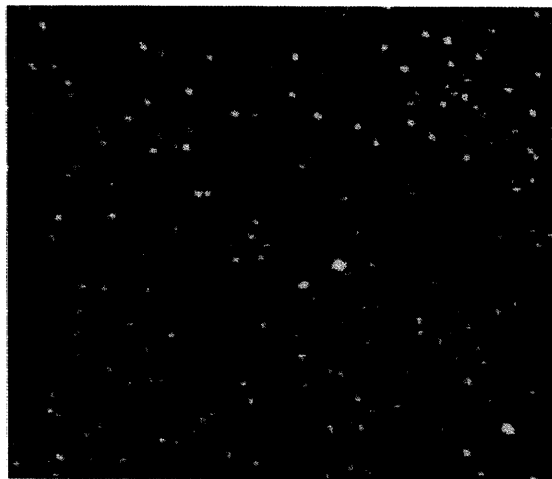


Fig. 2: (top) STM image of the Si(111)7x7 surface with adsorbed oxygen. The size of observed area is about $400 \text{\AA} \times 340 \text{\AA}$. Dark and bright spots are observed in this image, corresponding two kinds of adsorbed structure of oxygen. (bottom) conductance at point contact measured during oxygen exposure.

Moreover, we investigated the effect of the conductance on nanometer-size morphology of the surface. We measured the contact conductance on an epitaxially-grown Si island on the Si(111)7x7 surface, and compared it with that measured on flat area. Figure 3(top) is a typical STM image of the Si(111)7x7 surface with Si islands. We chose islands with the 7x7 structure on surface and measured the conductance on them. Figure 3(bottom) is a plot of conductance as a function of tip displacement from the tunneling condition, similar to that of Fig. 1. The contact conductance measured on the island is smaller than that obtained on terrace. We believe that it is due to the scattering of conducting electrons by steps surrounding the island, as is depicted in the inserted schematics. At the steps, the surface states are disrupted. The steps, therefore, cause electron scattering, reducing the conductance measured on the island. An interesting observation is that the conductance was reduced only on islands but not near surface steps. This means in order to obtain the reduced conductance, the contact area must be surrounded by surface steps in all directions. These observations also support our speculation that the conductance is due to the surface states. As the tip displacement increases further, the conductance

demonstrate that STM can be used to visualize electron scattering by steps or other kinds of defects on surfaces. As a sample, we used Au(111) and Cu(111) surfaces, both of which have two-dimensional electronic states localized on surface. Unlike silicon, gold and copper are metals, and thus they do not have a band gap at the Fermi energy. But, if looking at a plot of the projected bulk states onto a (111) plane of both surfaces written in an E-k (energy - wave number) space, there is a gap around the Fermi energy. Au(111) and Cu(111) have surface states in the gap;¹³⁾ so-called Shockley states. Since they are not coupled with the bulk states, two-dimensionally localized electronic states are formed on these surfaces. In the case of Au(111) and Cu(111) as well as Ag(111) surfaces, their two-dimensional electronic systems are supposed to be quite similar to that of free electrons because those systems show using ARPES parabolic and isotropic energy dispersion, similar to that of free electron, except an effective mass.¹³⁾

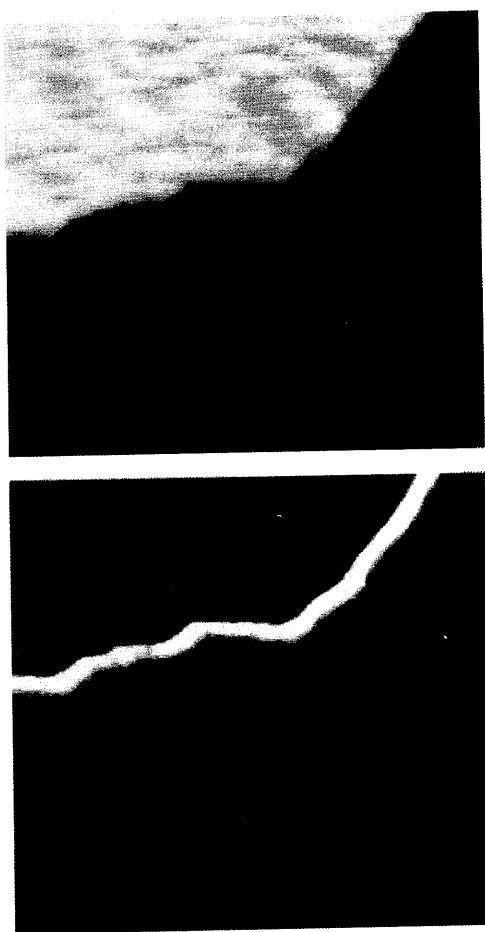


Fig. 4: STM (top) and STS (bottom, normalized dI/dV) images taken on the same area of Au(111) surface. The size of observed area is $320\text{\AA} \times 320\text{\AA}$. String-like features are observed in the STS image running parallel to the step edges (bright line) on the upper side of terrace.

For those electrons in the localized states, steps and other defects on the surfaces are regarded as a scattering center because they break the periodicity of atomic arrangement on surface. As a result of the scattering and interference of electrons, those structures make standing waves around them. It generates spatially oscillated structures in electronic density of states, and thus they can be detected and imaged using scanning tunneling

spectroscopy (STS). With STS, we observed standing waves around steps and defects on Au(111) and Cu(111) surfaces.¹⁴⁾ All measurements were performed with STM setups in a UHV chamber and at room temperature.

In STS experiments, we measured I-V spectra at each (or every a few) point during a scanning over the surface for the STM measurement. During the measurement of the I-V spectra, the feedback circuit for controlling the tip position was on hold. Bias voltage, which also determines the gap distance during the spectrum measurement, was kept rather high, $\sim +3\text{V}$, in order to avoid a fluctuation of the gap distance due to the change in density of states by standing wave formation. According to the 0th order approximation, tunneling conductance dI/dV is proportional to the density of states of the sample surface. For instance, the value of dI/dV at $+2\text{V}$ corresponds to the density of states of the surface at 2eV above the Fermi level. Images of dI/dV or normalized dI/dV ($(dI/dV)/(I/V)$), thus, displays a spatial distribution of density of states with a nanometer scale resolution. An image of dI/dV can also be obtained by applying a modulation voltage on the bias voltage and detecting its response in tunneling current with a lock-in amplifier. These three values, dI/dV , normalized dI/dV , and dI/dV by the modulation technique, are, however, slightly different in an interpretation of STS. This subject was discussed in detail elsewhere.¹⁵⁾

Figure 4 is an STM image (top) and an image of normalized dI/dV at a sample bias voltage of $+0.15\text{V}$ obtained with STS (bottom). The STS image was taken on the same area as the STM image. It corresponds to an image of the local density of states (LDOS) at $+0.15\text{eV}$ (empty state) above the Fermi energy. There is a monoatomic step in the upper portion. On the upper side of the step string-like features are observed running parallel to the step (bright line) in the STS image. These are peak positions of standing waves. Its period or separation between the string-like features ($\sim 15\text{\AA}$) is roughly equal to a half of the wave length of electronic states at $+0.15\text{eV}$ above the Fermi level. Although its amplitude is smaller than that of the upper side of steps factor of 5, the oscillatory structure can also be observed at the lower side of step. Paired line features observed all over the surface in the STM image are due to surface reconstruction, $22 \times \sqrt{3}$ structure of Au(111) surface. The structure does not seem to affect the pattern of standing waves as far as we observed.

Since the wave length of the electronic states depends on the energy level because of an energy dispersion, a period of the oscillatory structure also depends on the bias voltage at which dI/dV is calculated. Figure 5 is normalized dI/dV (STS) images at a bias voltage of $+0.15\text{V}$ (top), $+0.25\text{V}$, $+0.35\text{V}$, and $+0.45\text{V}$ (bottom), respectively. These correspond to the density-of-states at $+0.15\text{eV}$ to $+0.45\text{eV}$ above the Fermi level. The observed area is the upper right corner of the images in Fig. 4. The feature due to the surface reconstruction appears more clearly on an STS image of higher bias voltage. But, if one watches the features due to the standing waves along the step, you will find that the period of the standing waves changes with a bias voltage. Separation of the lines in these images become narrower with increasing a bias voltage (from the top to the bottom). This is because the electronic states with a higher energy have a shorter wave length. Therefore, these STS measurements can be used to determine the relation of energy and wave number, that is, an energy dispersion of the electronic states. We found that the experimentally obtained energy dispersion curve shows a

good agreement with the extrapolated one obtained by angle-resolved photoemission, which provides an energy dispersion curve of the filled states only.

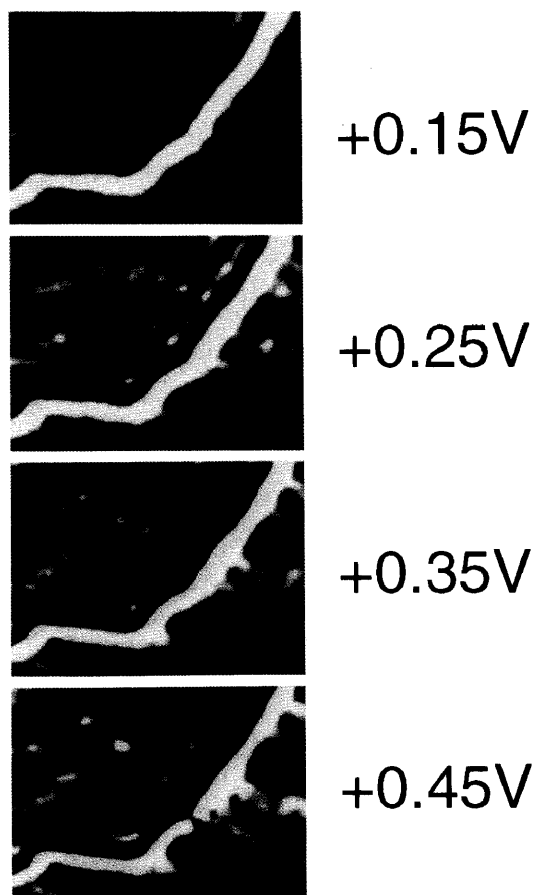


Fig. 5: Normalized dI/dV (STS) images at +0.15V, +0.25V, +0.35V, and +0.45V taken at the upper right corner of the area shown in the images of Fig. 4. These images show that the period of the standing waves decreases with an increase of sample bias voltage at which dI/dV is calculated. It is consistent with an energy dispersion of the states.

Standing waves are also formed around point defects. Figure 6 is an STM (top) and STS (bottom) images of an area including point defects, which are hardly seen in the STM image. Concentric ring features surrounding the point defects are observed in the STS image as well as linear features along the step edges. Circular standing waves indicate that the electronic states are isotropic to all directions, which is consistent with a result of angle-resolved photoemission spectroscopy.

We have tried a similar observation on Cu(111) surface, which has electronic states similar to that of Au(111) surface except its effective mass. The results are shown in Fig. 7. The top image is an STM image of the area including steps and point defects. Again, point defects are hardly visible in this STM image. The bottom one is the corresponding STS image (normalized dI/dV at +0.2V). Similar with the case of Fig. 6, concentric ring features around the point defects and linear features along step edges are observed.

From the images the showing standing waves, we can obtain information on scattering phenomena, which has been very important in an interpretation of electric

conduction or electron transport in the condensed matters. Recently, importance of scattering events by individual defects is more realized than before because conductors with a smaller size and longer mean free path have now become available. Using STS, we can obtain principal parameters of individual scattering events, such as scattering amplitude and phase shift. For instance, from the images in Fig. 4, we found that the amplitude of the standing waves at the upper side of the step edge is larger than that of lower side. This demonstrates clearly that the electrons from the upper side are scattered more strongly than those from the lower side. From the relative position of the step, or whether the step comes on a peak or bottom position in the standing waves, scattering phase shift can be measured directly and as a function of energy level of electrons. What we found for the Au(111) surface is that the phase shift depends on step orientation. $\langle 11\bar{2} \rangle$ and $\langle \bar{1}\bar{1}2 \rangle$ steps have phase shifts different by about $\pi/2$.

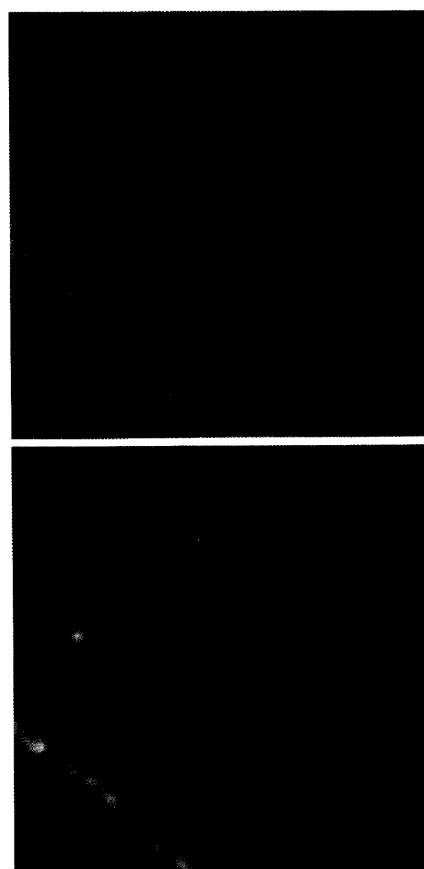


Fig. 6: STM (top) and STS (bottom, normalized dI/dV at +0.15V) images taken on Au(111) surface including a step and several point defects. The size of the observed area is about $120\text{\AA} \times 120\text{\AA}$. Concentric ring features due to standing waves are observed around the defect sites.

Information on how the standing waves decay with a distance from its scattering center tells us about coherence length of the electrons in the states. Coupling with bulk states or phonon scattering are possible sources of destroying the coherence. By analyzing a decay of the standing waves in details those processes could be investigated. In the case of Au(111) we observed, however, the standing waves decays much faster ($\sim 30\text{\AA}$) than expected

from these dephasing processes. This short decay length is due to a limited energy resolution by room temperature measurements. Because of the limited energy resolution ($\sim 3kT$), the observed standing waves become a mixture of those with a wave length in a finite range Δk , making the waves decay with a length of $1/\Delta k$.

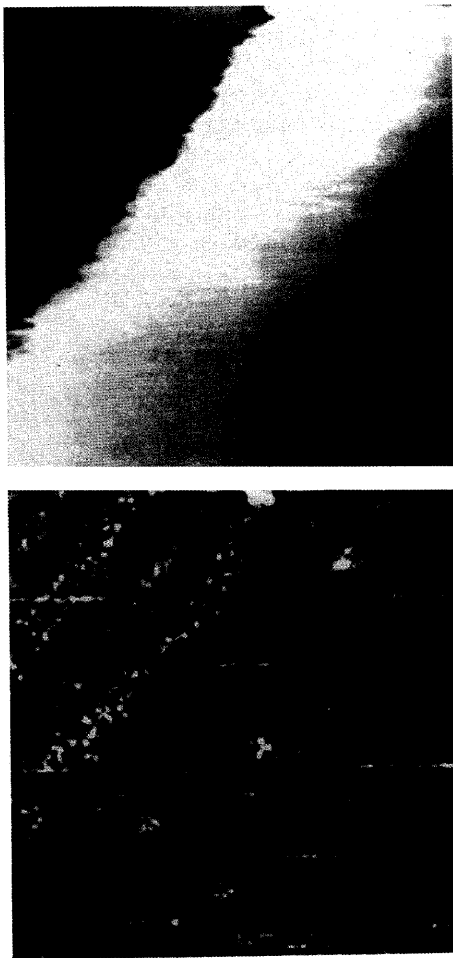


Fig. 7: STM (top) and STS (bottom, normalized dI/dV at $+0.2V$) images taken on Cu(111) surface simultaneously. The size of observed area is $80\text{\AA} \times 80\text{\AA}$. In the STS image, standing waves around point defects and step edges are observed. Measured period of the oscillatory structure is $\sim 14\text{\AA}$, which is in a good agreement with that expected from energy dispersion of the surface states.

4. Conclusion

By the two examples of semiconductor and metal surfaces, we have demonstrated that there are some electronic states which are localized on the surface and make a two dimensional electronic system, and that STM is a powerful tool to investigate properties of these 2D electron

system. It is found that in both cases nanoscale local structures such as steps, point defects, and adsorbates, have a significant effect on the behavior of the electronic system. Recent advance in surface science make it possible to arrange steps or adsorbates regularly with a nanometer scale in a macroscopic range. Of course, STM is also a very powerful tool for manipulating the arrangement of those structure in a nanometer scale. In addition to two dimensional systems we introduced in this paper, recently 1-dimensional electronic states localized on surface steps or in nanometer-wide terraces have been reported.^{16, 17)} With a help of technologies developed in surface science and STM, we expect that these unique low dimensional electron systems would provide us with new electronic devices in the near future.

[†]present address: Department of Physics, Yonsei University, Seoul, Korea

- 1) e.g. A. Zangwill: *Physics at Surfaces* (Cambridge Univ. Press, Cambridge, 1988).
- 2) K. Takayanagi, Y. Tanishiro, M. Takahashi, and S. Takahashi, *J. Vac. Sci. Technol.* **A3** (1985) 1502.
- 3) D.E. Eastman, F.J. Himpsel, J.A. Knapp, and K.C. Pandey, *Physics of Semiconductors* (Inst. of Phys., Bristol, 1978) p. 1059.
- 4) e.g. S. Datta: *Electronic Transport in Mesoscopic Systems* (Cambridge Univ. Press, Cambridge, 1995).
- 5) M.F. Crommie, C.P. Lutz and D.M. Eigler, *Science* **262** (1993) 218, *Nature* **363** (1993) 524.
- 6) U. Backes and H. Ibach, *Solid State Comm.* **40** (1981) 575.
- 7) B.N.J. Persson and J.E. Demuth, *Phys. Rev.* **B33** (1984) 5968; B.N.J. Persson, *Phys. Rev.* **B34** (1986) 5916.
- 8) M. Henzler: *Surface Physics of Materials* vol. 1, (Academic Press, New York, 1975) p.241.
- 9) Y. Hasegawa, I.-W. Lyo and Ph. Avouris, *Appl. Surf. Sci.* **76/77** (1994) 347, *Surf. Sci.* **358** (1996) 32.
- 10) C.-S. Jiang, X. Tong, S. Hasegawa, and S. Ino, *Surf. Sci.* submitted, cf. S. Hasegawa and S. Ino, *Phys. Rev. Lett.* **68** (1992) 1192.
- 11) I.-W. Lyo and Ph. Avouris, *Science* **253** (1991) 173.
- 12) In-Whan Lyo, Ph. Avouris, S. Schubert, and R. Hoffmann, *J. Phys. Chem.* **94** (1990) 4400, Ph. Avouris, In-Whan Lyo and F. Bozso, *J. Vac. Sci. Technol.* **B9** (1991) 424.
- 13) S.D. Kevan and G.H. Gayload, *Phys. Rev.* **B38** (1987) 5809.
- 14) Y. Hasegawa and Ph. Avouris, *Phys. Rev. Lett.* **71** (1993) 1071.
- 15) Y. Hasegawa and Ph. Avouris, *Jpn. J. Appl. Phys.* **33** (1994) 3675.
- 16) Ph. Avouris and I.-W. Lyo, *Science* **264** (1994) 942.
- 17) H. Namba, N. Nakanishi, T. Yamaguchi, T. Ohta, and H. Kuroda, *Surf. Sci.* **357/358** (1996) 238.